July 1976

AN ANALYSIS OF SATELLITE STATE VECTOR OBSERVABILITY USING SST TRACKING DATA

Thomas S. Englar, Jr.
and
Carol L. Hammond

FINAL REPORT
Contract NAS 5-20830

Prepared for

NATIONAL AERONAUTICS AND SPACE ADMINISTRATION
Goddard Space Flight Center
Greenbelt, Maryland 20771

BUSINESS AND TECHNOLOGICAL SYSTEMS, INC.
Aerospace Building
10210 Greenbelt Road
Seabrook, Maryland 20801

1. Report No.	2. Government Accession No.	3. Recipient's Catalog No.

4. Title and Subtitle	5. Report Date
AN ANALYSIS OF SATELLITE STATE VECTOR OBSERVABILITY USING SST TRACKING DATA	July 1976
	6. Performing Organization Code
7. Author(s) Thomas S. Englar, Jr. and Carol L. Hammond	8. Performing Organization Report No. BTS-TR-76-30
9. Performing Organization Name and Address Business and Technological Systems, Inc. Aerospace Building 10210 Greenbelt Road Seabrook, Maryland 20801	10. Work Unit No.
	11. Contract or Grant No. NAS 5-20830
12. Sponsoring Agency Name and Address NASA/Goddard Space Flight Center Greenbelt, Maryland 20771 Ms. Barbara Lowery	13. Type of Report and Period Covered Final Report
	14. Sponsoring Agency Code

15. Supplementary Notes

16. Abstract

Observability of satellite state vectors using only SST tracking data has been investigated by covariance analysis under a variety of satellite and station configurations. These results indicate very precarious observability in most short arc cases. The consequences of this are extremely large variances on many state components, such as the downrange component of the relay satellite position. As an illustration of the impact of observability problems, an example is given of two distinct satellite orbit pairs generating essentially the same data arc. The physical bases for unobservability are outlined and related to proposed TDRSS configurations. These results are relevant to any mission depending upon TDRSS to determine satellite state.

The required mathematical analysis and the software used is also described.

17. Key Words (Selected by Author(s))	18. Distribution Statement

19. Security Classif. (of this report)	20. Security Classif. (of this page)	21. No. of Pages	22. Price*
Unclassified	Unclassified		

*For sale by the Clearinghouse for Federal Scientific and Technical Information, Springfield, Virginia 22151.

TABLE OF CONTENTS

Page

I. INTRODUCTION....................I-1

II. PROGRAM DESCRIPTION....................II-1

2.1 Input....................II-2

2.2 Data....................II-4

2.3 Initialization....................II-6

2.4 Main Loop....................II-7

2.5 Output....................II-9

2.6 Main Program Listing....................II-10

2.7 Subroutine HCOMP....................II-16

2.8 Subroutine STATN....................II-19

2.9 Subroutine DSAMM....................II-22

2.10 Flow Chart....................II-23

III. NUMERICAL STUDIES....................III-1

Series I - 24 Hr. Equatorial Satellite and a Polar Satellite....................III-1

Series II - ATS-6 and GEOS-C....................III-22

An Example of Equivalence....................III-34

APPENDIX A - $(A'A)^{\dagger} = A^{\dagger}A^{\dagger\prime}$....................A-1

APPENDIX B - Sensitive or Normal?....................B-1

I. INTRODUCTION

This report presents the analysis techniques used in analysis of state vector observability obtained from SST data and describes software and numerical tests.

All facets of the program are idealized in that the Earth is represented by a point mass, there are no transmission delays at the satellites, and all measurements are instantaneous. These implications mean that the sofware runs quickly, has small core requirements, and has easily specified input. It also means in general that errors are smaller than in a real world problem with modeling errors. Hence the program can be used easily to determine feasibility.

The conclusions of the numerical work indicate that for short arcs - less than 0.5 km - there is not complete observability. For arcs longer than 1 km errors are on the order of 100 m, however modeling errors at this arc length may become very important.

II. PROGRAM DESCRIPTION

This program is designed to analyze state observability with SST tracking through the use of a simple, spherical earth program.

All facets of the problem are idealized, in that the Earth is represented by a point mass, there are no transmission delays at the satellites, and all measurements are instantaneous.

2.1 Input: Input consists of:

Coordinates of the Station:

θ_S = Station Longitude (deg)

λ_S = Station Latitude (deg)

Coordinates of the Relay Satellite:

a = Orbit Semimajor Axis (km)

e = Orbit Eccentricity

i = Orbit Inclination (deg)

Ω = Longtiude of Ascending Mode (deg)

ω = Argument of Perigee (deg)

ϕ = Initial True Anomaly. (deg)

Coordinates of Tracked Satellite:

Same as Relay Satellite.

Parameters of the Data Arc:

Δ = Interval Between Readings (sec)

N = Number of Readings

Print Controls:

IP1 = 1 Print ρ sensitivity matrix.

IP2 = 1 Print $\dot{\rho}$ sensitivity matrix

IP3 = 1 Print ρ information matrix

IP4 = 1 Print $\dot{\rho}$ information matrix

IP5 = 1 Print ρ projection matrix

IP6 = 1 Print $\dot{\rho}$ projection matrix

IP7 = 1 Print ρ covariance matrix

IP8 = 1 Print $\dot{\rho}$ covariance matrix

IP9 = 1 Print ρ correlation matrix

IP10 = 1 Print $\dot{\rho}$ correlation matrix

IP11 = 1 Print combined projection matrix

IP12 = 1 Print combined covariance matrix

IP13 = 1 Print combined correlation matrix

IP14 = 1 Print inverse of ρ information matrix

IP15 = 1 Print inverse of $\dot{\rho}$ information matrix

Visibility Criteria:

CTAN = Cutoff angle to relay satellite (deg)

CTDS = Minimum distance between earth and intersatellite LOS (km)

2.2 Data: The following parameters are in block data:

π = 3.1415926536

ω_e = 0.72921159E-4 rad/sec Earth's rotation rate

μ = 398601. km^3/sec^2 Earth's gravitational constant

R_E = 6378. km Earth radius

In the desired inertial system,

$$
\begin{aligned}
x^0 &= x_e \cos \Omega - y_e \sin \Omega \\
y^0 &= x_e \sin \Omega + y_e \cos \Omega \\
z^0 &= z_e \\
\dot{x}^0 &= \dot{x}_e \cos \Omega - \dot{y}_e \sin \Omega \\
\dot{y}^0 &= \dot{x}_e \sin \Omega + \dot{y}_e \cos \Omega \\
\dot{z}^0 &= \dot{z}_e .
\end{aligned}
$$

This is done for each satellite and we denote the relay satellite position and velocity by (r_1, v_1) and the tracked satellite by (r_2, v_2).

2.3 Initialization: After input, the positions and velocities of the station, and both satellites are computed in an inertial system coinciding with the Earth-Center-Fixed (ECF) system at time zero. The station initialization is detailed in the description of subroutine STATN.

To initialize the satellites, we first define the magnitude of the radius vector,

$$r = \frac{a(1-e^2)}{1+e \cos \phi} \quad ;$$

then the radial speed,

$$\dot{r} = e \sin \phi \sqrt{\frac{\mu}{p}} \;, \; p = a(1-e^2) \quad ;$$

and then tangential speed,

$$r\dot{\phi} = \sqrt{\mu p}/r \quad .$$

In a cartesian orbit plane coordinate system with $\hat{x}$ through the ascending node and $\hat{z}$ along the angular momentum vector, we have

$$\begin{aligned}
x_0 &= r \cos (\phi+\omega) \\
y_0 &= r \sin (\phi+\omega) \\
z_0 &= 0 \\
\dot{x}_0 &= \dot{r} \cos (\phi+\omega) - r\dot{\phi} \sin (\phi+\omega) \\
\dot{y}_0 &= \dot{r} \sin (\phi+\omega) + r\dot{\phi} \cos (\phi+\omega) \\
\dot{z}_0 &= 0.
\end{aligned}$$

In a cartesian, equatorial coordinate system with $\hat{x}$ through the ascending node, we have

$$\begin{aligned}
x_e &= x_0 \\
y_e &= y_0 \cos i \\
z_e &= y_0 \sin i \\
\dot{x}_e &= \dot{x}_0 \\
\dot{y}_e &= \dot{y}_0 \cos i \\
\dot{z}_e &= \dot{y}_0 \sin i.
\end{aligned}$$

2.4 Main Loop: The main body of code is executed N times, once for each time point. The purpose of the main body of code is the generation of the N by 12 matrices S_1 and S_2 defined by:

$$i^{th} \text{ row of } S_1 = \frac{\partial\rho(t_i)}{\partial r_1(0), v_1(0), r_2(0), v_2(0)}$$

$$i^{th} \text{ row of } S_2 = \frac{\partial\dot{\rho}(t_i)}{\partial r_1(0), v_1(0), r_2(0), v_2(0)}$$

This is implemented in several steps. First, using subroutine STATN, the current position and velocity $(r_0(t_i), v_0(t_i))$ of the station are computed. Then, using subroutine DSAMM, the current position and velocity of each satellite $(r_1(t_i), v_1(t_i))$, $(r_2(t_i), v_2(t_i))$ as well as the state transition matrices

$$\Psi_1 = \frac{\partial r_1(t_i), v_1(t_i)}{\partial r_1(0), v_1(0)}$$

$$\Psi_2 = \frac{\partial r_2(t_i), v_2(t_i)}{\partial r_2(0), v_2(0)}$$

are calculated.

Then, in subroutine HCOMP, the matrices

$$H_{11} = \frac{\partial\rho(t_i)}{\partial r_1(t_i), v_1(t_i)}$$

$$H_{12} = \frac{\partial\rho(t_i)}{\partial r_2(t_i), v_2(t_i)}$$

$$H_{21} = \frac{\partial\dot{\rho}(t_i)}{r_1(t_i), v_1(t_i)}$$

$$H_{22} = \frac{\partial\dot{\rho}(t_i)}{\partial r_2(t_i), v_2(t_i)}$$

The i^{th} rows of S_1 and S_2 are then computed in the main body of code by

$$i^{th} \text{ row of } S_1 = [H_{11}\ \Psi_1,\ H_{12}\ \Psi_2]$$

$$i^{th} \text{ row of } S_2 = [H_{21}\ \Psi_1,\ H_{22}\ \Psi_2] \quad .$$

2.5 Output: Because this program will be used to explore observability, there are a large number of output processes.

The sensitivity matrices S_1 and S_2 can be printed.

The information matrices

$$W_1 = S_1^T R_1^{-1} S_1$$

and

$$W_2 = S_2^T R_2^{-1} S_2$$

where R_1 and R_2 are the measurement noises on range and range rate, respectively, can be printed.

The projection matrices

$$P_1 = S_1^\dagger S_1$$

$$P_2 = S_2^\dagger S_2$$

and

$$P_3 = \begin{bmatrix} S_1 \sigma_1^{-1} \\ S_2 \sigma_2^{-1} \end{bmatrix}^\dagger \begin{bmatrix} S_1 \sigma_1^{-1} \\ S_2 \sigma_2^{-1} \end{bmatrix} ,$$

can be printed. These matrices are very important for determining the observable space since they are identity matrices on that space.

The "covariance matrices" $W_1^\dagger$, $W_2^\dagger$, and $W_3^\dagger = (W_1+W_2)^\dagger$ can be printed. "Covariance" is in quotes here because singularity of these matrices does *not* imply perfect information.

The "correlation" matrices obtained from $W_1^\dagger$, $W_2^\dagger$, and $W_3^\dagger$ can be printed.

```
      PROGRAM SST(INPUT,OUTPUT,TAPE5=INPUT,TAPE6=OUTPUT)
C***                TSS IS THE STATION LONGITUDE (IN DEGREES)
C***                XLAMS IS THE STATION LATITUDE (IN DEGREES)
C***                TAS IS THE LONGITUDE OF THE RELAY SATELLITE (IN DEGREES)
C***                B IS THE SEMI-MAJOR AXIS OF THE TRACKED SATELLITE ORBIT
C***                   (IN KILOMETERS)
C***                TTS IS THE STARTING ANGLE OF THE TRACKED SATELLITE
C***                   (IN DEGREES)
C***                DELT IS THE MEASUREMENT INTERVAL
C***                N IS THE NUMBER OF MEASUREMENTS (N)100)
      COMMON/INVAL/PI,OME,ZMU,A,RE
      COMMON/ONE/TT,TA,TS,XLAM,G(6,6),TIME,B,DELT,P0(6),
     * S1(100,12),S2(100,12),H11(1,6),H12(1,6),H21(1,6),H22(1,6),
     * TMP1(1,6),TMP2(1,6),W1(100,12),W2(100,12),
     * SW1(12,12),AFLAG(12),ATEMP(12),SW2(12,12),
     * P1(6),OMGA,TMAT(6,6),ST(6,6),XNU,TVEC(6),QT(6,6),T(6,6),TTR(6,6),
     * P2(6)
      COMMON NC(72),IN,IO
      COMMON EMU,AIJ(3,3),BIJ(3,3),CIJ(3,3),DIJ(3,3),THET,BETAM1,
     * G0,G1,G2,G3,G4,G5,G6,G7,F0,F1,F2,F3,F4,F5,F6,F7,00A,PSI2(6,6)
      COMMON SR1,SR2,BETAT2,SD1,SD2
      DIMENSION COMB(200,12),C1(200,12)
      DIMENSION TARC(12)
      DIMENSION APSG(12)
      DIMENSION P00(6),P10(6),P20(6)
      DIMENSION PSI1(6,6)
      DTOR=PI/180.E0
C**   READ IN STATION COORDINATES
      READ(5,10)TSS,XLAMS,FF
C**   READ IN RELAY COORDINATES
      READ(5,10)A1,E1,RI1,BOM1,RLOM1,PHI1
C**   READ IN TRACKED SATELLITE COORDINATES
      READ(5,10)A2,E2,RI2,BOM2,RLOM2,PHI2
C**   READ IN ARC TIMING
      READ(5,15)DELT,N
C**   READ PRINT CONTROLS
      READ(5,20)IP1,IP2,IP3,IP4,IP5,IP6,IP7,IP8,IP9,IP10,IP11,IP12,IP13,
     * IP14,IP15,IP16,IP17,IP18,IP19,IP20
20    FORMAT(20I1)
C**   READ NOISE SIGMAS
      READ(5,10)SIGR,SIGRD
C**   READ IN VISIBILITY CRITERIA
      READ(5,10)CTAN,CTDS
C**   READ IN APRIORI SIGMAS
      READ(5,12)(APSG(I),I=1,12)
12    FORMAT(6E10.4)
C***  READ IN ARC ENDPOINTS
      READ(5,12)(TARC(I),I=1,12)
      WRITE(6,50)TSS,XLAMS,FF
      WRITE(6,55)A1,E1,RI1,BOM1,RLOM1,PHI1
      WRITE(6,60)A2,E2,RI2,BOM2,RLOM2,PHI2
      WRITE(6,65)DELT,N
      WRITE(6,111)SIGR,SIGRD
      WRITE(6,112)CTAN,CTDS
      WRITE(6,113)(APSG(I),I=1,12)
```

```
      WRITE(6,114)(TARC(I),I=1,12)
111   FORMAT(5X,*SIGR,SIGRD*/2E20.8)
112   FORMAT(5X,*CTAN,CTDS*/2E20.8)
C
113   FORMAT(5X,*APSG(1-6)*/6E20.8/5X,*APSG(7-12)*/6E20.8)
114   FORMAT(5X,*TARC(1-6)*/6E20.8/5X,*TARC(7-12)*/6E20.8/*1*)
50    FORMAT(*1*,4X,*TSS,XLAMS,FF*/3E20.8)
55    FORMAT(5X,*A1,E1,RI1,BOM1,RLOM1,PHI1*/6E20.8)
60    FORMAT(5X,*A2,E2,RI2,BOM2,RLOM2,PHI2*/6E20.8)
65    FORMAT(5X,*DELT,N*/E20.8,I5)
C***          INITIALIZATIONS
      FF=1.-FF
      CTAN=CTAN*DTOR
      P=A1*(1.-E1*E1)
      PHI1=PHI1*DTOR
      R=P/(1.+E1*COS(PHI1))
      RD=E1*SIN(PHI1)*SQRT(ZMU/P)
      RPHD=SQRT(ZMU*P)/R
      PHPOM = PHI1 + RLOM1*DTOR
      C=COS(PHPOM)
      S=SIN(PHPOM)
      P1(1)=R*C
      P1(4)=RD*C-RPHD*S
      P1(2)=R*S
      P1(5)=RD*S+RPHD*C
      C=COS(RI1*DTOR)
      S=SIN(RI1*DTOR)
      P10(3)=P1(2)*S
      P10(6)=P1(5)*S
      P1(2)=P1(2)*C
      P1(5)=P1(5)*C
      C=COS(BOM1*DTOR)
      S=SIN(BOM1*DTOR)
      P10(1)=P1(1)*C-P1(2)*S
      P10(4)=P1(4)*C-P1(5)*S
      P10(2)=P1(1)*S+P1(2)*C
      P10(5)=P1(4)*S+P1(5)*C
      WRITE(6,55)P10
      P=A2*(1.-E2*E2)
      PHI2=PHI2*DTOR
      R=P/(1.+E2*COS(PHI2))
      RD=E2*SIN(PHI2)*SQRT(ZMU/P)
      RPHD=SQRT(ZMU*P)/R
      PHPOM = PHI2 + RLOM2*DTOR
      C=COS(PHPOM)
      S=SIN(PHPOM)
      P2(1)=R*C
      P2(4)=RD*C-RPHD*S
      P2(2)=R*S
      P2(5)=RD*S+RPHD*C
      C=COS(RI2*DTOR)
      S=SIN(RI2*DTOR)
      P20(3)=P2(2)*S
      P20(6)=P2(5)*S
      P2(2)=P2(2)*C
```

```
      P2(5)=P2(5)*C
      C=COS(BOM2*DTOR)
      S=SIN(BOM2*DTOR)
      P20(1)=P2(1)*C-P2(2)*S
      P20(4)=P2(4)*C-P2(5)*S
      P20(2)=P2(1)*S+P2(2)*C
      P20(5)=P2(4)*S+P2(5)*C
      WRITE(6,55)P20
      TS=TSS*DTOR
      XLAM=XLAMS*DTOR
      CL= COS(XLAM)
      OMGA=OME
      P00(1)=RE*COS(TS)*CL
      P00(2)=RE*SIN(TS)*CL
      P00(3)=RE*SIN(XLAM)
      P00(4)=-OMGA*P00(2)
      P00(5)=OMGA*P00(1)
      P00(6)=0.
      P0(6)=0.
      P0(3)=P00(3)
      NAP=0
      DO 431 I=1,12
      IF(APSG(I).EQ.0.0)GO TO 431
      NAP=NAP+1
      DO 432 K=1,12
      S1(NAP,K)=0.0
  432 S2(NAP,K)=0.0
      S1(NAP,I)=SIGR/APSG(I)
      S2(NAP,I)=SIGRD/APSG(I)
  431 CONTINUE
      IARC=1
      I1=NAP
      J=0
C**
C**   START OF MAIN LOOP
C**
      DO 1000 I=1,N
   24 TIME=J*DELT+TARC(IARC)
      J=J+1
      IF(TIME.LE.TARC(IARC+1))GO TO 25
      IARC=IARC+2
      IF(TARC(IARC).GE.1.E30)GO TO 26
      J=0
      GO TO 24
   25 CONTINUE
      CALL STATN(P0,P00,OMGA,TIME)
      TOBAR=0.
      CALL DSAMM(TIME,TOBAR,P10,P10(4),P1,P1(4),0,2)
      DO 23 JJ=1,6
      DO 23 KK=1,6
      PSI1(JJ,KK)=PSI2(JJ,KK)
   23 CONTINUE
      CALL DSAMM(TIME,TOBAR,P20,P20(4),P2,P2(4),0,2)
      CALL VIS(P0,P1,P2,CTAN,CTDS,ISEE)
      IF(ISEE.EQ.0)GO TO 1000
```

```
      I1=I1+1
      CALL MCOMP(FF)
      DO 70 K=1,6
      K6=K+6
      S1(I1,K) =0.E0
      S1(I1,K6)=0.E0
      S2(I1,K) =0.E0
      S2(I1,K6)=0.E0
      DO 70 L=1,6
      S1(I1,K)=S1(I1,K) + H11(1,L) * PSI1(L,K)
      S1(I1,K6)=S1(I1,K6)+ H12(1,L) * PSI2(L,K)
      S2(I1,K)= S2(I1,K) + H21(1,L) * PSI1(L,K)
      S2(I1,K6)=S2(I1,K6)+ H22(1,L) * PSI2(L,K)
70    CONTINUE
      IF(I1.EQ.100)GO TO 26
1000  CONTINUE
26    CONTINUE
C**
C**   END MAIN LOOP
      WRITE(6,15)TIME,I1
      N1=I1
      IF(IP1.NE.1)GO TO 401
      WRITE(6,200)((S1(I,J),J=1,6),I=1,N1)
      WRITE(6,225)
      WRITE(6,200)((S1(I,J),J=7,12),I=1,N1)
401   CONTINUE
      IF(IP2.NE.1)GO TO 402
      WRITE(6,250)
      WRITE(6,200)((S2(I,J),J=1,6),I=1,N1)
      WRITE(6,225)
      WRITE(6,200)((S2(I,J),J=7,12),I=1,N1)
      WRITE(6,250)
10    FORMAT(3E20.8)
15    FORMAT(E20.8,I5)
200   FORMAT(6E20.8)
225   FORMAT(5(/))
250   FORMAT(10(/))
402   CONTINUE
      DO 110 I=1,N1
      DO 110 J=1,12
      S1(I,J)=S1(I,J)/SIGR
      S2(I,J)=S2(I,J)/SIGRD
      W1(I,J)=S1(I,J)
      W2(I,J)=S2(I,J)
      COMB(I,J)=S1(I,J)
      CI(I,J) = COMB(I,J)
      IF(I.LE.NAP)GOTO 110
      I2 = N1 + I - NAP
       COMB(I2,J) = S2(I,J)
      CI(I2,J) = COMB(I2,J)
110   CONTINUE
      IF(IP3.NE.1)GO TO 410
      CALL SMALT(N1,S1,S1,SW1,100,12)
      CALL SPRNT(SW1)
      IF(IP14.NE.1)GO TO 410
```

```
      CALL GINV2(SW1,SW2,AFLAG,ATEMP,12,12,12,1.E-10,DET)
      CALL SPRNT(SW1)
410   IF(IP4.NE.1)GO TO 411
      CALL SMULT(N1,S2,S2,SW1,100,12)
      CALL SPRNT(SW1)
      IF(IP15.NE.1)GO TO 411
      CALL GINV2(SW1,SW2,AFLAG,ATEMP,12,12,12,1.E-10,DET)
      CALL SPRNT(SW1)
411   CONTINUE
      CALL GINV2(S1,SW1,AFLAG,ATEMP,100,N1,12,1.E-10,DET)
      CALL GINV2(S2,SW1,AFLAG,ATEMP,100,N1,12,1.E-10,DET)
      IF(IP5.NE.1)GO TO 405
      CALL SMULT(N1,S1,N1,SW1,100,12)
      CALL SPRNT(SW1)
405   CONTINUE
      IF(IP6.NE.1)GO TO 406
      CALL SMULT(N1,S2,W2,SW1,100,12)
      CALL SPRNT(SW1)
406   CONTINUE
      CALL SMULT(N1,S1,S1,SW1,100,12)
      IF(IP7.NE.1)GO TO 412
      CALL SPRNT(SW1)
412   IF(IP9.NE.1)GO TO 413
      DO 415 I=1,12
      SQ=SQRT(SW1(I,I))
      IF(SQ.EQ.0.0)GO TO 415
      DO 417 J=1,12
      IF(J.GE.I)GO TO 416
      SW1(I,J)=SW1(I,J)/SQ
      GO TO 417
416   SW1(J,I)=SW1(J,I)/SQ
417   CONTINUE
      SW1(I,I)=1.
415   CONTINUE
      CALL SPRNT(SW1)
413   CALL SMULT(N1,S2,S2,SW1,100,12)
      IF(IP8.NE.1)GO TO 420
      CALL SPRNT(SW1)
420   IF(IP10.NE.1)GO TO 421
      DO 465 I=1,12
      SQ=SQRT(SW1(I,I))
      IF(SQ.EQ.0.0)GO TO 465
      DO 467 J=1,12
      IF(J.GE.I)GO TO 466
      SW1(I,J)=SW1(I,J)/SQ
      GO TO 467
466   SW1(J,I)=SW1(J,I)/SQ
467   CONTINUE
      SW1(I,I)=1.
465   CONTINUE
      CALL SPRNT(SW1)
421   CONTINUE
      N2=N1+N1-GAP
      CALL GINV2(COMB,SW1,AFLAG,ATEMP,200,N2,12,1.E-10,DET)
      IF(IP11.NE.1)GO TO 423
```

```
      CALL SMULT(N2,COMB.C1.SW1,200,12)
      CALL SPRNT(SW1)
  423 CALL SMULT(N2.COMB.COMB.SW1,200,12)
      IF(IP12.NE.1)GO TO 427
      CALL SPRNT(SW1)
  427 IF(IP13.NE.1)STOP
      DO 495 I=1,12
      SQ=SQRT(SW1(I,I))
      IF(SQ.EQ.0.0)GO TO 495
      DO 497 J=1,12
      IF(J.GE.I)GO TO 496
      SW1(I,J)=SW1(I.J)/SQ
      GO TO 497
  496 SW1(J,I)=SW1(J,I)/SQ
  497 CONTINUE
      SW1(I,I)=1.
  495 CONTINUE
      CALL SPRNT(SW1)
      STOP
      END
```

2.7 Subroutine HCOMP

Purpose: To compute the sensitivities of the current range and range rate readings with respect to the current twelve-dimensional state.

Analysis: Let

$$(r_0, v_0) = (x_0, y_0, z_0, \dot{x}_0, \dot{y}_0, \dot{z}_0)$$

$$(r_1, v_1) = (x_1, y_1, z_1, \dot{x}_1, \dot{y}_1, \dot{z}_1)$$

$$(r_2, v_2) = (x_2, y_2, z_2, \dot{x}_2, \dot{y}_2, \dot{z}_2)$$

denote the inertial position and velocity (state) vectors of, respectively, the station, the relay satellite, and the tracked satellite at the current time.

The data readings at the current time are range,

$$\rho = |r_1 - r_0| + |r_2 - r_1| = \rho_{10} + \rho_{21}$$

and range rate

$$\dot{\rho} = \frac{(v_1 - v_0) \cdot (r_1 - r_0)}{\rho_{10}} + \frac{(v_2 - v_1) \cdot (r_2 - r_1)}{\rho_{21}}$$

$$= \dot{\rho}_{10} + \dot{\rho}_{21} .$$

The sensitivity matrices are

$$\frac{\partial \rho}{\partial r_1, v_1} = H_{11} = \left[\frac{x_1-x_0}{\rho_{10}} - \frac{x_2-x_1}{\rho_{21}} , \frac{y_1-y_0}{\rho_{10}} - \frac{y_2-y_1}{\rho_{21}} , \right.$$

$$\left. \frac{z_1-z_0}{\rho_{10}} - \frac{z_2-z_1}{\rho_{21}} , 0 , 0 , 0 \right] ;$$

$$\frac{\partial\rho}{\partial r_2, v_2} = H_{12} = \left[\frac{x_2 - x_1}{\rho_{21}} \ , \ \frac{y_2 - y_1}{\rho_{21}} \ , \ \frac{z_2 - z_1}{\rho_{21}} \ , \ 0 \ , \ 0 \ , \ 0 \right];$$

$$\frac{\partial\dot{\rho}}{\partial r_1, v_1} = H_{21} = \left[\frac{\dot{x}_1 - \dot{x}_0}{\rho_{10}} - \frac{\dot{x}_2 - \dot{x}_1}{\rho_{21}} - \frac{\dot{\rho}_{10}}{\rho_{10}} \frac{x_1 - x_0}{\rho_{10}} + \frac{\dot{\rho}_{21}}{\rho_{21}} \frac{x_2 - x_1}{\rho_{21}} \right. ,$$

$$\frac{\dot{y}_1 - \dot{y}_0}{\rho_{10}} - \frac{\dot{y}_2 - \dot{y}_1}{\rho_{21}} - \frac{\dot{\rho}_{10}}{\rho_{10}} \frac{y_1 - y_0}{\rho_{10}} + \frac{\dot{\rho}_{21}}{\rho_{21}} \frac{y_2 - y_1}{\rho_{21}} ,$$

$$\frac{\dot{z}_1 - \dot{z}_0}{\rho_{10}} - \frac{\dot{z}_2 - \dot{z}_1}{\rho_{21}} - \frac{\dot{\rho}_{10}}{\rho_{10}} \frac{z_1 - z_0}{\rho_{10}} + \frac{\dot{\rho}_{21}}{\rho_{21}} \frac{z_2 - z_1}{\rho_{21}} ,$$

$$\left. h_{111} \ , \ h_{112} \ , \ h_{113} \right];$$

$$\frac{\partial\dot{\rho}}{\partial r_2, v_2} = H_{22} = \left[\frac{\dot{x}_2 - \dot{x}_1}{\rho_{21}} - \frac{\dot{\rho}_{21}}{\rho_{21}} \frac{x_2 - x_1}{\rho_{21}} \right. ,$$

$$\frac{\dot{y}_2 - \dot{y}_1}{\rho_{21}} - \frac{\dot{\rho}_{21}}{\rho_{21}} \frac{y_2 - y_1}{\rho_{21}} , \quad \frac{\dot{z}_2 - \dot{z}_1}{\rho_{21}} - \frac{\dot{\rho}_{21}}{\rho_{21}} \frac{z_2 - z_1}{\rho_{21}} ,$$

$$\left. h_{121} \ , \ h_{122} , \ h_{123} \right] .$$

```
      SUBROUTINE HCOMP(FF)
      COMMON/INVAL/PI,OME,ZMU,A,RE
      COMMON/ONE/TT,TA,TS,XLAM,Q(6,6),TIME,B,DELT,P0(6),
     * S1(100,12),S2(100,12),H11(1,6),H12(1,6),H21(1,6),H22(1,6),
     *  TMP1(1,6),TMP2(1,6),W1(100,12),W2(100,12),
     * SW1(12,12),AFLAG(12),ATEMP(12),SW2(12,12),
     * P1(6),OMGA,TMAT(6,6),ST(6,6),XNU,TVEC(6),QT(6,6),T(6,6),TTR(6,6),
     *  P2(6)
      EQUIVALENCE  (P0(1),X0),(P0(2),Y0),(P0(3),Z0),
     *             (P1(1),X1),(P1(2),Y1),(P1(3),Z1),
     *             (P2(1),X2),(P2(2),Y2),(P2(3),Z2),
     *             (P0(4),XD0),(P0(5),YD0),(P0(6),ZD0),
     *             (P1(4),XD1),(P1(5),YD1),(P1(6),ZD1),
     *             (P2(4),XD2),(P2(5),YD2),(P2(6),ZD2)
      X10=X1-X0
      X21=X2-X1
      Y10=Y1-Y0
      Y21=Y2-Y1
      Z10=Z1-Z0
      Z21=Z2-Z1
      XD10=XD1-XD0
      XD21=XD2-XD1
      YD10=YD1-YD0
      YD21=YD2-YD1
      ZD10=ZD1-ZD0
      ZD21=ZD2-ZD1
      R01=  SQRT(X10**2  + Y10**2  + Z10**2)
      R12=  SQRT(X21**2  + Y21**2  + Z21**2)
      SH21=(X10*XD10 + Y10*YD10 + Z10*ZD10) /R01
      SH22=(X21*XD21 + Y21*YD21 + Z21*ZD21) /R12
      WRITE(6,20)R01,R12,SH21,SH22
20    FORMAT(4E20.8//)
      DO 10 J=1,6
      H11(1,J)=0.E0
      H12(1,J)=0.E0
10    CONTINUE
      H11(1,1)=FF*X10/R01 - X21/R12
      H11(1,2)=FF*Y10/R01 - Y21/R12
      H11(1,3)=FF*Z10/R01 - Z21/R12
      H12(1,1)=  X21/R12
      H12(1,2)=  Y21/R12
      H12(1,3)=  Z21/R12
      H21(1,1)=FF*XD10/R01-XD21/R12-FF*SH21/R01*X10/R01+SH22/R12*X21/R12
      H21(1,2)=FF*YD10/R01-YD21/R12-FF*SH21/R01*Y10/R01+SH22/R12*Y21/R12
      H21(1,3)=FF*ZD10/R01-ZD21/R12-FF*SH21/R01*Z10/R01+SH22/R12*Z21/R12
      H21(1,4)=H11(1,1)
      H21(1,5)=H11(1,2)
      H21(1,6)=H11(1,3)
      H22(1,1)= XD21/R12 - SH22/R12*X21/R12
      H22(1,2)= YD21/R12 - SH22/R12*Y21/R12
      H22(1,3)= ZD21/R12 - SH22/R12*Z21/R12
      H22(1,4)= H12(1,1)
      H22(1,5)= H12(1,2)
      H22(1,6)= H12(1,3)
      RETURN
      END
```

2.8 Subroutine STATN

Purpose: To compute the inertial position and velocity of the station at the current time.

Analysis: Let

$$(r_0, v_0) = (x_0, y_0, z_0, \dot{x}_0, \dot{y}_0, \dot{z}_0)$$

denote the inertial position and velocity of the station at the current time. The Earth-center-fixed (ECF) coordinates of the station are input in terms of latitude λ_S (spherical earth) and longitude θ_S, so the initial ECF criteria coordinates of the station are

$$R_E \cos \theta_S \cos \lambda_S$$

$$R_E \sin \theta_S \cos \lambda_S$$

$$R_E \sin \lambda_S \quad ,$$

where R_E is the Earth radius.

Because the inertial coordinate system coincides with the ECF system at t = 0, the inertial cartesian coordinates of the station at time zero are

$$x_0^0 = R_E \cos \theta_S \cos \lambda_S$$

$$y_0^0 = R_E \sin \theta_S \cos \lambda_S$$

$$z_0^0 = R_E \sin \lambda_S$$

$$\dot{x}_0^0 = - \omega_e \, y_0^0$$

$$\dot{y}_0^0 = \omega_e \, x_0^0$$

$$\dot{z}_0^0 = 0$$

where ω_e is the inertial rotation rate of the Earth.

The inertial cartesian coordinates of the station at the current time, t, are then given by

$$x_0 = x_0^0 \cos \omega_e t - y_0^0 \sin \omega_e t$$

$$y_0 = x_0^0 \sin \omega_e t + y_0^0 \cos \omega_e t$$

$$z_0 = z_0^0$$

$$\dot{x}_0 = - \omega_e y_0$$

$$\dot{y}_0 = \omega_e x_0$$

$$\dot{z}_0 = 0 .$$

```
SUBROUTINE STATN(PO,POO,OMGA,TIME)
DIMENSION PO(6),POO(6)
WT=OMGA*TIME
C=COS(WT)
S=SIN(WT)
PO(1)=POO(1)*C-POO(2)*S
PO(2)=POO(1)*S+POO(2)*C
PO(4)=-OMGA*PO(2)
PO(5)=OMGA*PO(1)
RETURN
END
```

2.9 Subroutine DSAMM

Purpose: To propagate the six-dimensional state vector and to compute the six by six transition matrix.

Analysis: The state vector is propagated by the closed form, nonlinear, two-body solution. The transition matrix is computed by the closed form representation for perturbations about the two-body orbit.

2.10 Flowchart

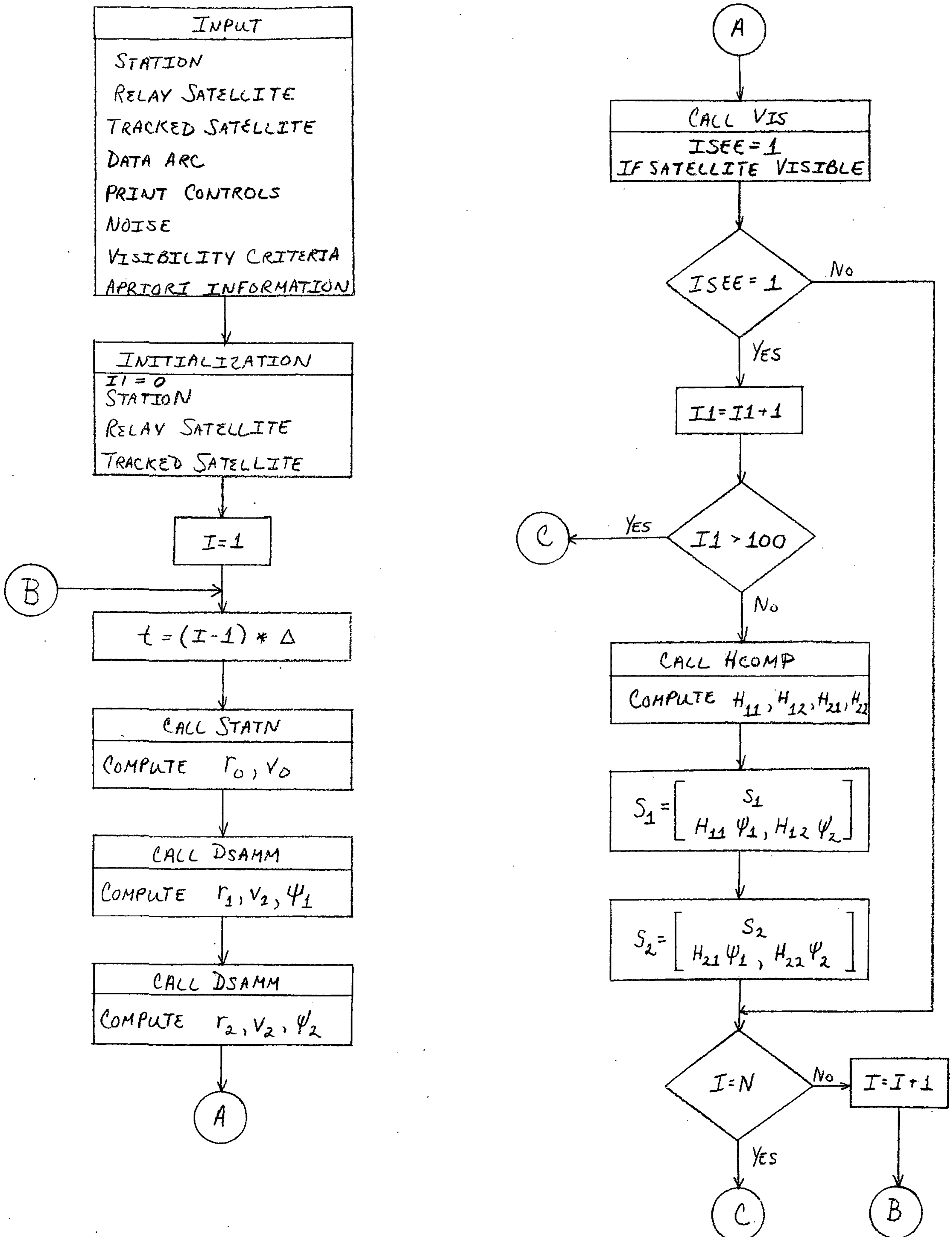

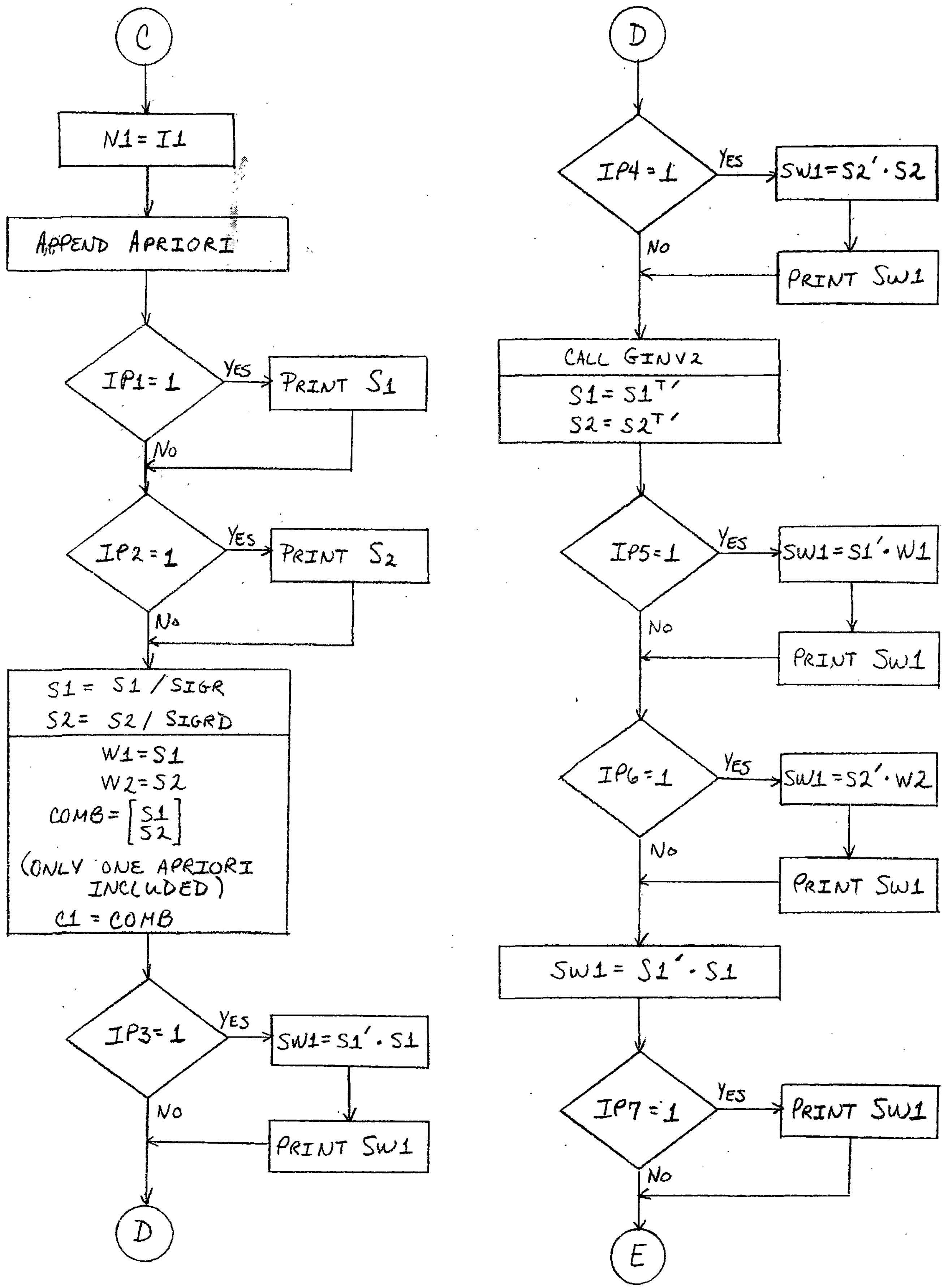
C
N1 = I1
APPEND APRIORI
IP1 = 1
YES
PRINT S1
NO
IP2 = 1
YES
PRINT S2
NO
S1 = S1 / SIGR
S2 = S2 / SIGRD
W1 = S1
W2 = S2
COMB = [S1 S2]
(ONLY ONE APRIORI INCLUDED)
C1 = COMB
IP3 = 1
YES
SW1 = S1′ · S1
NO
PRINT SW1
D
D
IP4 = 1
YES
SW1 = S2′ · S2
NO
PRINT SW1
CALL GINV2
S1 = S1T′
S2 = S2T′
IP5 = 1
YES
SW1 = S1′ · W1
NO
PRINT SW1
IP6 = 1
YES
SW1 = S2′ · W2
NO
PRINT SW1
SW1 = S1′ · S1
IP7 = 1
YES
PRINT SW1
NO
E

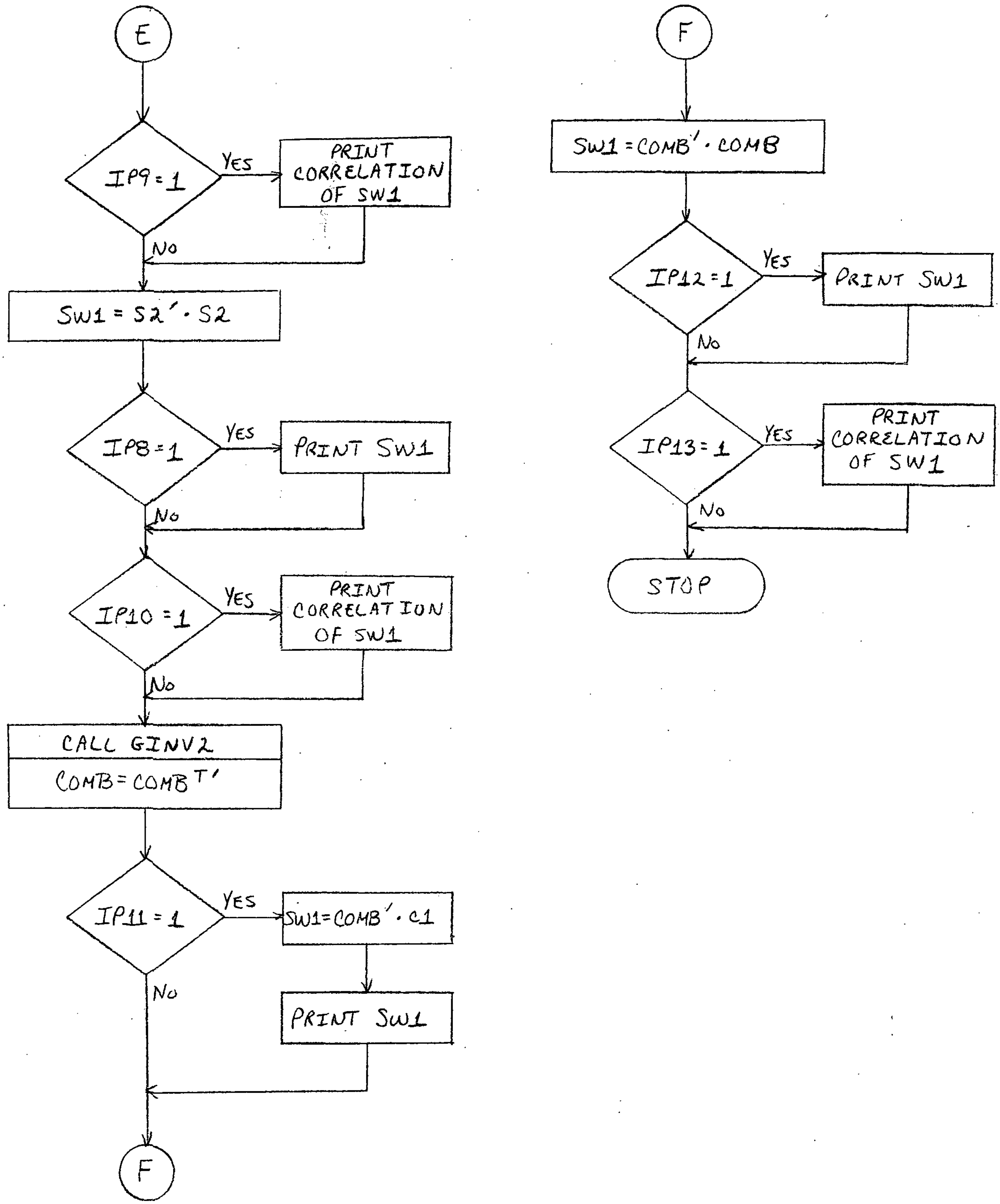
E
IP9 = 1
YES
PRINT CORRELATION OF SW1
NO
SW1 = S2′ · S2
IP8 = 1
YES
PRINT SW1
NO
IP10 = 1
YES
PRINT CORRELATION OF SW1
NO
CALL GINV2
COMB = COMBT′
IP11 = 1
YES
SW1 = COMB′ · C1
PRINT SW1
NO
F
F
SW1 = COMB′ · COMB
IP12 = 1
YES
PRINT SW1
NO
IP13 = 1
YES
PRINT CORRELATION OF SW1
NO
STOP

III. NUMERICAL STUDIES

In these studies the measurement noise was given a standard deviation of 3m (range) and 1 mm/sec (range rate).

Rosman was taken at -82.88 longitude
35.20 latitude
Mojave was taken at -116.89 longitude
35.33 latitude
ATS-6 was taken at -94° longitude in Series I.

SERIES I:

In this series a geosynchronous relay satellite was used with a tracked satellite in circular, polar orbit at about 840 km altitude. Experiments were made with station location and with the relative positions of the satellites.

Case 1. Equatorial station directly under relay satellite, both on x-axis. Tracked satellite starts at south pole (-z-axis), with velocity along y-axis. Tracked satellite was tracked for one period (≈6100 sec). Observability rank = 9.

In this configuration, there is complete negative correlation between the relay satellite z-component and the tracked satellite x-component. From the projection matrix, we find that the observable combination of z_1 and x_2 is

$$\begin{bmatrix} .028 \\ -.166 \end{bmatrix}$$

Thus a perturbation

$$\begin{bmatrix} \Delta z_1 \\ \Delta x_2 \end{bmatrix} = \begin{bmatrix} 0.166 \\ 0.028 \end{bmatrix} \lambda$$

is unobservable. This perturbation ratio corresponds very closely to

$$\begin{bmatrix} a_1 \\ a_2 \end{bmatrix} = \begin{bmatrix} 42164 \\ 7213 \end{bmatrix}$$

(where a_1 and a_2 are the orbit semi-major axes), indicating that a rotation of the orbit planes about the line of nodes (y-axis) is unobservable. This accounts for a rank decrement of one.

There is also complete correlation between the relay satellite $\dot{z}$-component and the tracked satellite y- and $\dot{z}$-components. From the projection matrix we find that the observable space is spanned by

$$\begin{bmatrix} .99999982 & -.43925539E-6 \\ -.42620828E-3 & -.0010306110 \\ -.43925539E-6 & .99999894 \end{bmatrix}$$

From this it follows that any vector

$$\begin{bmatrix} \Delta\dot{z}_1 \\ \Delta y_2 \\ \Delta\dot{z}_2 \end{bmatrix} = \begin{bmatrix} 1 \\ 2346.267763 \\ 2.418092003 \end{bmatrix} \lambda$$

is unobservable. This seems very much as if y_2 is directly unobservable. However, the units here are km and km/sec which means that the components are of about equal importance. In fact this perturbation corresponds very closely to a rotation of the orbits about the x-axis, that is to a change of

$$\begin{bmatrix} \Delta\dot{z}_1 \\ \Delta y_2 \\ \Delta\dot{z}_2 \end{bmatrix} = \begin{bmatrix} 3.0388 \\ 7213. \\ 7.4338 \end{bmatrix} \sin i$$

There is also correlation between y_1, $\dot{x}_1$, and $\dot{x}_2$ with

$$\begin{bmatrix} \Delta\dot{y}_1 \\ \Delta\dot{x}_1 \\ \Delta\dot{x}_2 \end{bmatrix} = \begin{bmatrix} .72921157E-4 & .17630615E-3 \\ 1. & -.12855708E-7 \\ -.12855708E-7 & .99999997 \end{bmatrix}$$

being observable and therefore

$$\begin{bmatrix} \Delta y_1 \\ \Delta \dot{x}_1 \\ \Delta \dot{x}_2 \end{bmatrix} = \begin{bmatrix} 1 \\ -.7292E-4 \\ .1763E-3 \end{bmatrix} \lambda$$

being unobservable. This perturbation corresponds very closely to

$$\begin{bmatrix} a_1 \\ v_1 \\ v_2 \end{bmatrix} = \begin{bmatrix} 42164 \\ -3.0388 \\ -7.4338 \end{bmatrix} \sin \alpha \quad ,$$

i.e. a rotation of both orbits about the z-axis.

Thus we see that small rotations of the axis system are unobservable for this case.

Observability is the same with range, range-rate, or both.

The variances in this case cannot be determined because the information matrix is singular. However the "variances" appearing in the generalized inverse of the information matrix are lower bounds for the recovered variances. These gave standard deviations as shown in Table 1. One of the principal observations from this table is that combining different data types having different correlation structure can improve statistics far beyond the expectation on the basis of the increased number of observations.

These variances are unrealistically low, of course, because of pseudoinversion; they do show, however, the variances that can be expected on the observable subspaces. To gain an idea of actual variances, a priori standard deviations of 100 km were put on satellite positions with the results shown in Table 2. These are all larger of course. They show that, while only a three dimensional subspace is unobservable mathematically, as a practical matter, very little is observable. The following variables are unobservable in any realistic sense:

Variable	Standard Deviation		
	Range	Range-Rate	Combined
x_1	.047 km	4.069 km	.002 km
y_1	.000 km	.000 km	.000 km
z_1	.013 km	.027 km	.001 km
$\dot{x}_1$	.056 m/s	.168 m/s	.002 m/s
$\dot{y}_1$	.126 m/s	.523 m/s	.006 m/s
$\dot{z}_1$	.192 m/s	.816 m/s	.013 m/s
x_2	.080 km	.157 km	.004 km
y_2	.000 km	.000 km	.000 km
z_2	.086 km	.201 km	.005 km
$\dot{x}_2$	.079 m/s	.473 m/s	.004 m/s
$\dot{y}_2$	.065 m/s	.107 m/s	.004 m/s
$\dot{z}_2$	.046 m/s	.028 m/s	.004 m/s

Case 1. Standard Deviations Without A Priori

Table 1

Variable	Standard Deviation		
	Range	Range-Rate	Combined
x_1	.048 km	4.065 km	.002 km
y_1	100.000 km	100.000 km	100.000 km
z_1	98.568 km	98.568 km	98.568 km
$\dot{x}_1$	7.292 m/s	7.294 m/s	7.292 m/s
$\dot{y}_1$	.127 m/s	.522 m/s	.006 m/s
$\dot{z}_1$	42.627 m/s	42.634 m/s	42.627 m/s
x_2	16.862 km	16.863 km	16.862 km
y_2	100.000 km	100.000 km	100.000 km
z_2	.086 km	.201 km	.005 km
$\dot{x}_2$	17.631 m/s	17.637 m/s	17.631 m/s
$\dot{y}_2$	.065 m/s	.107 m/s	.004 m/s
$\dot{z}_2$	103.061 m/s	103.061 m/s	103.061 m/s

Case 1. Standard Deviation Using A Priori

Table 2

Relay satellite	downrange	(y_1)
	crossrange	(z_1)
	radial velocity	($\dot{x}_1$)
	crossrange velocity	($\dot{z}_1$)
Tracked satellite	downrange	(y_2)
	crossrange	(x_2)
	radial velocity	($\dot{z}_2$)
	crossrange velocity	($\dot{x}_2$)

Naturally, much of the problem is caused by the very poor geometry of the station and satellites.

Case 2. This case is the same as Case 1 except for an eccentricity of 0.012 on the relay satellite. This gave a rank of 10 because the combination (y_1, $\dot{x}_1$, $\dot{x}_2$) (rotation about the z-axis) was recoverable. However, the variance on y_1 is very large and the errors project onto $\dot{x}_1$ and $\dot{x}_2$.

Variable	Standard Deviation		
	Range	Range-Rate	Combined
x_1	0.105 km	4.168 km	0.005 km
y_1	6330. km	3148. km	3133. km
z_1	0.030 km	0.026 km	0.001 km
$\dot{x}_1$	4556. m/s	226. m/s	225. m/s
$\dot{y}_1$	0.916 m/s	0.525 m/s	0.047 m/s
$\dot{z}_1$	1.522 m/s	0.829 m/s	0.071 m/s
x_2	0.177 km	0.157 km	0.008 km
y_2	0.618 km	0.065 km	0.000 km
z_2	0.173 km	0.204 km	0.010 km
$\dot{x}_2$	11030. m/s	548. m/s	546. m/s
$\dot{y}_2$	0.111 m/s	0.108 m/s	0.007 m/s
$\dot{z}_2$	0.069 m/s	0.028 m/s	0.005 m/s

Case 2. Standard Deviations

Table 3

Case 3. Rosman station. Tracked satellite starts at south pole (-z-axis), with velocity along y-axis. Tracked satellite was tracked for one period (≈6100 sec). Observability rank = 11 and 12.

Standard Deviations for this run are shown in Table 4. They indicate how precarious observability is for this configuration. The unobservable subspace using range rate is the same as that noted in Case 1 as being equivalent to a rotation about the z-axis, i.e.

$$\begin{bmatrix} \Delta y_1 \\ \Delta \dot{x}_1 \\ \Delta \dot{x}_2 \end{bmatrix} = \begin{bmatrix} 1 \\ -.7292E-4 \\ -.1763E-3 \end{bmatrix} \lambda \ .$$

In Table 5 are shown the standard deviations for the same configuration with a priori standard deviations of 100 km on satellite positions.

We see that the same variables as in Case 1 are still unobservable in any practical sense:

Relay satellite	downrange	(y_1)
	crossrange	(z_1)
	radial velocity	$(\dot{x}_1)$
	crossrange velocity	$(\dot{z}_1)$
Tracked satellite	downrange	(y_2)
	crossrange	(x_2)
	radial velocity	$(\dot{z}_2)$
	crossrange velocity	$(\dot{x}_2)$

Results tracking from Mojave were qualitatively the same. However, the change in geometry gave demonstrable benefits in the most unobservable subspace (y_1, $\dot{x}_1$, $\dot{x}_2$). In these components, which have the largest variances, the errors were halved while the remaining errors were essentially unchanged (Table 4.2). Note that this improvement is essentially the ratio of the aspect angle of Mojave (22°) compared with the aspect angle of Rosman (11°).

Variable	Standard Deviation		
	Range	Range-Rate	Combined
x_1	1435. km	75. km	74.619 km
y_1	395982. km	.000 km	21436.028 km
z_1	79462. km	4375. km	4363.806 km
$\dot{x}_1$	28959. m/s	4.582 m/s	1567.691 m/s
$\dot{y}_1$	94. m/s	5.631 m/s	5.616 m/s
$\dot{z}_1$	1671. m/s	88.475 m/s	88.237 m/s
x_2	13597. km	745.593 km	746.542 km
y_2	3859. km	202.687 km	202.141 km
z_2	11. km	.737 km	.735 km
$\dot{x}_2$	69820. m/s	.878 m/s	3780.034 m/s
$\dot{y}_2$	7. m/s	.458 m/s	.457 m/s
$\dot{z}_2$	3973. m/s	208.657 m/s	208.095 m/s

Case 3. Standard Deviations Without A Priori

Table 4.1

Variable	Standard Deviation		
	Range	Range-Rate	Combined
x_1	1453. km	76. km	75.675 km
y_1	200071. km	.000 km	10843.268 km
z_1	80448. km	4435. km	4422.330 km
$\dot{x}_1$	14503. m/s	4.727 m/s	786.007 m/s
$\dot{y}_1$	93. m/s	5.593 m/s	5.577 m/s
$\dot{z}_1$	1738. m/s	91.810 m/s	91.559 m/s
x_2	13767. km	758.729 km	756.628 km
y_2	4012. km	210.318 km	209.744 km
z_2	11. km	.730 km	.728 km
$\dot{x}_2$	35268. m/s	.897 m/s	1910.983 m/s
$\dot{y}_2$	7. m/s	.454 m/s	.453 m/s
$\dot{z}_2$	4130. m/s	216.516 m/s	215.925 m/s

Case 3. Standard Deviation Without A Priori (Mojave)

Table 4.2

Variable	Standard Deviation		
	Range	Range-Rate	Combined
x_1	4.976 km	4.514 km	2.683 km
y_1	99.981 km	100.000 km	98.518 km
z_1	98.285 km	98.430 km	55.288 km
$\dot{x}_1$	7.634 m/s	7.303 m/s	7.203 m/s
$\dot{y}_1$	1.313 m/s	.539 m/s	.512 m/s
$\dot{z}_1$	42.784 m/s	7.276 m/s	6.820 m/s
x_2	16.548 km	16.839 km	9.327 km
y_2	94.937 km	16.735 km	15.306 km
z_2	.537 km	.203 km	.182 km
$\dot{x}_2$	17.515 m/s	17.637 m/s	17.335 m/s
$\dot{y}_2$	.293 m/s	.108 m/s	.098 m/s
$\dot{z}_2$	97.849 m/s	17.237 m/s	15.771 m/s

Case 3. Standard Deviations With A Priori

Table 5

Case 4. The same as Case 3 except that a longer tracking arc was used, tracking for about five orbits (~9 hr). Observability rank = 11 and 12.

The unobservable space using range-rate is still the z-axis rotation,

$$\begin{bmatrix} \Delta y_1 \\ \Delta \dot{x}_1 \\ \Delta \dot{x}_2 \end{bmatrix} = \begin{bmatrix} 1 \\ -.7292E-4 \\ -.1763E-3 \end{bmatrix} \lambda$$

The standard deviations for this arc are shown in Table 6. Notice that the errors are beginning now to be reasonable, although still far greater than the measurement noise. These errors are small enough however so that a run with 100 km position a priori causes no significant change in the Range or combined tracking results.

Variable	Standard Deviation		
	Range	Range-Rate	Combined
x_1	.043 km	.012 km	.011 km
y_1	5.582 km	.000 km	1.414 km
z_1	.759 km	.883 km	.177 km
$\dot{x}_1$	.411 m/s	.001 m/s	.104 m/s
$\dot{y}_1$	.001 m/s	.000 m/s	.0002 m/s
$\dot{z}_1$	.083 m/s	.023 m/s	.022 m/s
x_2	.130 km	.033 km	.030 km
y_2	.194 km	.054 km	.052 km
z_2	.001 km	.000 km	.0002 km
$\dot{x}_2$	.983 m/s	.001 m/s	.249 m/s
$\dot{y}_2$	.002 m/s	.000 m/s	.0002 m/s
$\dot{z}_2$	.200 m/s	.056 m/s	.053 m/s

Case 4. Standard Deviations Without A Priori
10 hr. Arc

Table 6

Case 5: A comparison was made between the recovery possible when the tracked satellite orbit is in plan view and when it is "end-on". Because of visibility constraints, this comparison was made on a half-orbit arc. The end-on orbit started the tracked satellite over the south pole with velocity along the x-axis.

Overall recovery was better for the plan view orbit in the sense that: The largest variances (y_1 and $\dot{y}_2$) were in the end-on recovery; only x_1, $\dot{z}_1$, y_2 and $\dot{x}_2$ had smaller variances in the end-on recovery; and the smallest variances z_2 and $\dot{y}_2$) were in the plan recovery. Downrange velocity and radial position of the tracked satellite had the lowest variances in both cases.

Case 6: In this and the following case, an attempt was made to discover the effect of increased relay satellite a priori. The runs were made with the tracked orbit in plan view, Rosman station, a 30 second sampling interval over 2790 records (94 data points), and a priori standard deviations on the relay of 10m and 1 mm/sec.

The standard deviations were:

	σ_x	σ_y	σ_z
r	26 m	393 m	159 m
r-r	5 m	96 m	35 m
comb	4 m	88 m	31 m

From this we see that range-rate is a very much better data type than range, at this level of relay uncertainty. When the standard deviations on the relay x, y, and z were increased individually to 100 m, the following results were obtained.

$\sigma_x = 100$

	σ_x	σ_y	σ_z
r	74 m	1698 m	469 m
r-r	6 m	96 m	35 m
comb	5 m	96 m	34 m

$\sigma_y = 100$

	σ_x	σ_y	σ_z
r	26 m	434 m	160 m
r-r	9 m	127 m	76 m
comb	6 m	97 m	54 m

$\sigma_z = 100$

	σ_x	σ_y	σ_z
r	29 m	408 m	162 m
r-r	18 m	96 m	35 m
comb	15 m	89 m	32 m

These results show that for this tracking geometry, range-rate is a better data type and is less sensitive to relay satellite position errors.

When the standard deviations on the relay satellite were increased at one time to 100 m and 10 mm/sec, the following results were obtained.

	σ_x	σ_y	σ_z
r	76 m	1701 m	480 m
r-r	20 m	145 m	85 m
comb	19 m	144 m	84 m

Case 7: This is the same as Case 6 except that the tracked orbit is in end-on view. For the reference run, the standard deviations were:

	σ_x	σ_y	σ_z
r	25 m	689 m	69 m
r-r	6 m	80 m	6 m
comb	6 m	79 m	6 m

Again, it appears that range rate is a far superior data type than range. When the standard deviations on relay x, y and z were increased individually to 100 m, the following results were obtained.

$\sigma_x = 100$

	σ_x	σ_y	σ_z
r	108 m	762 m	118 m
r-r	9 m	83 m	7 m
comb	6 m	80 m	6 m

$\sigma_y = 100$ m

	σ_x	σ_y	σ_z
r	26 m	847 m	82 m
r-r	22 m	434 m	24 m
comb	14 m	294 m	17 m

$\sigma_z = 100$ m

	σ_x	σ_y	σ_z
r	26 m	690 m	70 m
r-r	18 m	80 m	6 m
comb	15 m	79 m	6 m

These results continue to bear out the superiority of range-rate data; however, they do not indicate that range-rate is less sensitive to relay position errors in this configuration.

When the standard deviations on the relay satellite were increased at one time to 100 m and 100 mm/sec, the following results were obtained.

	σ_x	σ_y	σ_z
r	112 m	1064 m	127 m
r-r	41 m	708 m	39 m
comb	38 m	688 m	37 m

Basically cases 6 and 7 indicate that for short arcs in this high-inclination satellite orbit, range-rate is a significantly better data type than range. Further, there appears to be an overall tendency for range rate to be somewhat less sensitive to relay errors than is range data.

Case 8: In this case we examined the effect of inclination of the tracked satellite orbit on tracked satellite recovery. For this purpose we used the conditions of Case 7 (end-on orbit) and gradually decreased the inclination. Figure 1 shows the standard deviation of the position recovery. The z-recovery becomes increasingly poor as inclination decreases and when the orbit is equatorial, sensitivity to cross-track components is zero.

Notice that this inertial parameterization (rather than HCL) appears to be a natural one in that uncertainties in x and y are virtually constant while z grows. If HCL were used, y and z would change from cross track and radial at $i = 90°$ to radial and cross track at $i = 0°$.

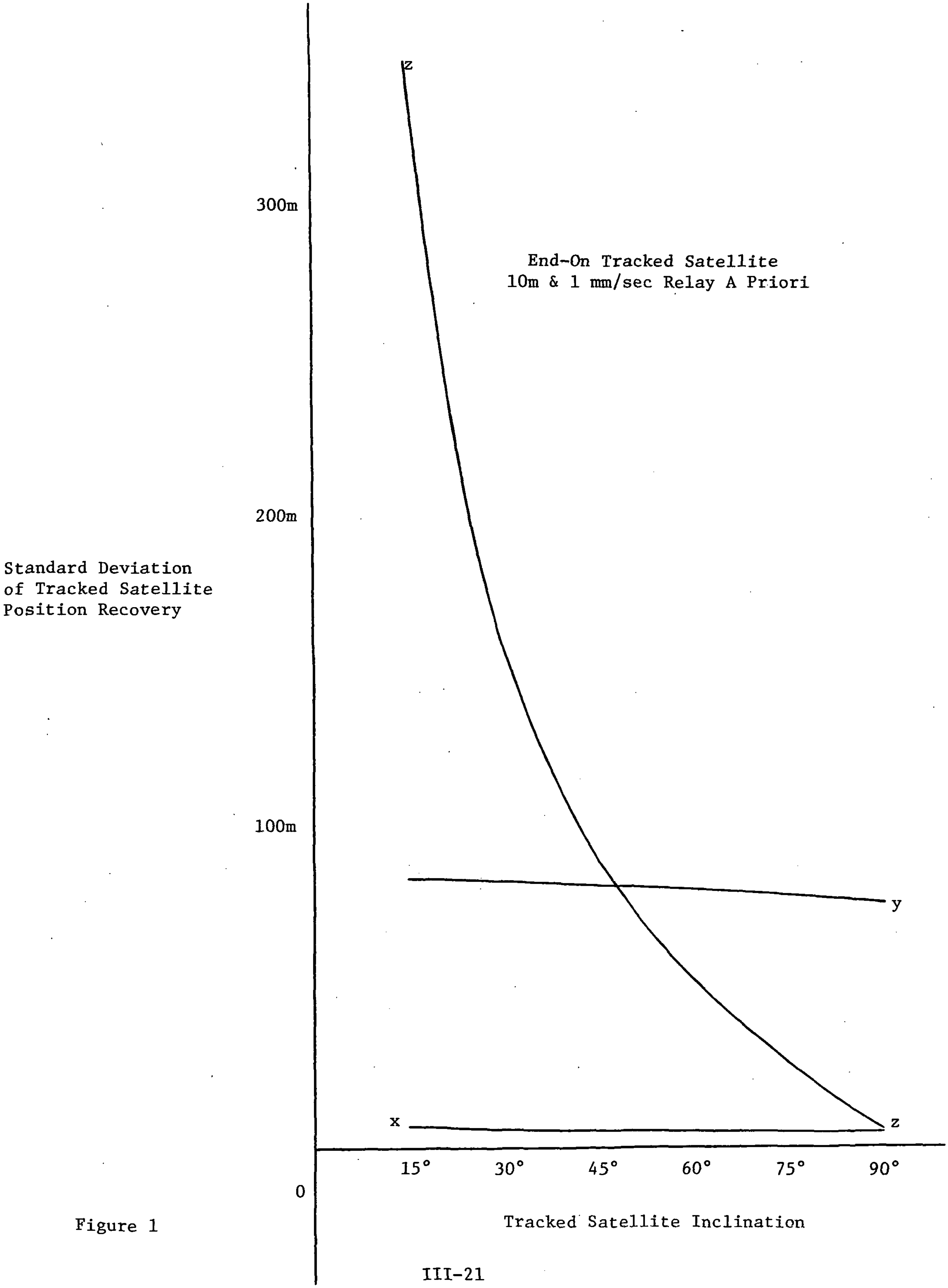

z
300m
200m
100m
0
End-On Tracked Satellite
10m & 1 mm/sec Relay A Priori
Standard Deviation
of Tracked Satellite
Position Recovery
y
x
z
15°
30°
45°
60°
75°
90°
Tracked Satellite Inclination

Figure 1

SERIES II: This series had ATS-6 and GEOS-C in various configurations.

ATS-6 was defined by

$a = 42164.18909$ km

$e = 0.000387768$

$i = 0.875423°$

$\Omega = 120.909439°$ $(257.894711°)$

$\omega = 109.629318°$

$\phi = 129.398243°$

GEOS-C was defined by:

$a = 7213.103$ km

$e = 0.001313909$

$i = 144.871022$

$\Omega = 153.618899°$ $(290.604171°)$

$\omega = 93.839036°$

$\phi = 190.876765°$

Case 1: Sampling interval 300 sec. Arc length 10.4 hours. This called for 125 data points, but because of visibility constraints collected only 81.

Observability Rank = 12.

The standard deviations using Rosman station are shown in Table 7. When the number of data points was increased while keeping arc length fixed, the improvement, particularly in the least recoverable components, was only slightly better than would be expected on the basis of $\sqrt{N}$. Hence the relative magnitudes of the numbers in Table 7 appear to be approximately correct for this arc, even with continuous tracking.

The standard deviations using Mojave station appear in Table 8. Using combined data, there is an improvement of nearly 50% as the case in Series I would lead us to expect. This improvement, however, is not uniform between range and range rate. Presumably this is caused by the aspect of GEOS in this case.

The correlation structure in all of the cases up to this point has been very poor, with the $y_1 - \dot{x}_1$ correlation (downrange distance-radial speed) being about -0.99999 from Mojave and about -0.999998 from Rosman. Some of the following cases are directed toward trying to remove this high correlation.

Variable	Standard Deviation		
	Range	Range Rate	Combined
x_1	.038 km	.027 km	.009 km
y_1	3.580 km	348.592 km	.967 km
z_1	.418 km	.455 km	.090 km
$\dot{x}_1$	.264 m/s	25.409 m/s	.071 m/s
$\dot{y}_1$	.002 m/s	.006 m/s	.000 m/s
$\dot{z}_1$	.052 m/s	.019 m/s	.015 m/s
x_2	.127 m/s	15.084 km	.033 km
y_2	.355 km	24.393 km	.099 km
z_2	.050 km	.031 km	.014 km
$\dot{x}_2$	.321 m/s	34.270 m/s	.087 m/s
$\dot{y}_2$	.488 m/s	50.251 m/s	.131 m/s
$\dot{z}_2$	.069 m/s	.074 m/s	.014 m/s

Case 1. Standard Deviations - Rosman

TABLE 7

Variable	Standard Deviation		
	Range	Range Rate	Combined
x_1	.036 km	.026 km	.010 km
y_1	2.172 km	390.291 km	.517 km
z_1	.467 km	.104 km	.087 km
$\dot{x}_1$	.154 m/s	28.449 m/s	.037 m/s
$\dot{y}_1$	.002 m/s	.007 m/s	.000 m/s
$\dot{z}_1$	.066 m/s	.036 m/s	.017 m/s
x_2	.151 km	16.812 km	.033 km
y_2	.035 km	27.357 km	.006 km
z_2	.064 km	.026 km	.015 km
$\dot{x}_2$	.215 m/s	36.110 m/s	.051 m/s
$\dot{y}_2$	.350 m/s	56.250 m/s	.084 m/s
$\dot{z}_2$	.072 m/s	.041 m/s	.016 m/s

Case 1. Standard Deviations - Mojave

TABLE 8

Case 2: Sampling interval 10 min. Arc length 24 hours. Because of visibility constraints, only 96 points were collected. The standard deviations are shown in Table 9. We can see that the variances are approaching acceptable levels. In addition, the correlations have decreased. The y_1 - $\dot{x}_1$ correlation while still high (-0.99986) has improved considerably from (-0.99999).

The achieved variances noted in Table 9 are, of course, unduly optimistic because of the presence of significant modelling errors.

Variable	Standard Deviation		
	Range	Range-Rate	Combined
x_1	.008 km	.008 km	.000 km
y_1	.288 km	118.658 km	.067 km
z_1	.080 km	.149 km	.024 km
$\dot{x}_1$	.021 m/s	8.649 m/s	.005 m/s
$\dot{y}_1$	.000 m/s	.002 m/s	.000 m/s
$\dot{z}_1$	.005 m/s	.005 m/s	.001 m/s
x_2	.024 km	5.134 km	.006 km
y_2	.026 km	8.305 km	.006 km
z_2	.006 km	.009 km	.002 km
$\dot{x}_2$	.029 m/s	10.984 m/s	.007 m/s
$\dot{y}_2$	.039 m/s	17.105 m/s	.009 m/s
$\dot{z}_2$	.014 m/s	.026 m/s	.004 m/s

Case 2. Standard Deviations, 24 Hour Arc - Rosman

TABLE 9

Case 3: In another effort to increase the accuracy of recovery, the eccentricity of the relay satellite (ATS-6) was increased to 0.1 and the run condition of Case 1 repeated. The results are shown in Table 10. Comparing these errors with those in Tables 7 and 8 it can be seen that the increase in eccentricity does indeed aid the recovery. However, the most significant reduction is in the down-range recovery from range-rate only. Aside from this, it appears simpler merely to use the Mojave station.

Variable	Standard Deviation		
	Range	Range-Rate	Combined
x_1	.051 km	.013 km	.012 km
y_1	2.532 km	4.730 km	.747 km
z_1	.451 km	.989 km	.079 km
$\dot{x}_1$	.168 m/s	.307 m/s	.050 m/s
$\dot{y}_1$	.012 m/s	.025 m/s	.004 m/s
$\dot{z}_1$	.091 m/s	.048 m/s	.027 m/s
x_2	.148 km	.333 km	.037 km
y_2	.369 km	.420 km	.109 km
z_2	.045 km	.042 km	.015 km
$\dot{x}_2$	.232 m/s	.453 m/s	.067 m/s
$\dot{y}_2$	.291 m/s	.619 m/s	.086 m/s
$\dot{z}_2$	.172 m/s	.197 m/s	.043 m/s

Case 3. Standard Deviations

Table 10

Case 4: A question that arises very quickly is the effect of knowledge of the relay satellite. In this case, a priori sigmas of 10 m and 1 mm/s were assumed for ATS and a 10.4 hour tracking arc used from Rosman. The standard deviations appear in Table 11 and we see that GEOS errors are down to the 2m, 2 mm/s level.

Along with this, the correlation structure is greatly improved. Also note that range-rate appears to be a better data type than range.

This result indicated that much shorter data arcs could be used, so an arc of 3.5 hours at a sample interval of 100 seconds was attempted. This gave excellent results with good correlation and maximum standard deviation of 6 m and 6 mm/s (range only). Again range rate was a better data type, (3 m and 2 mm/s).

Pushing this still further, a one hour data arc was attempted with a 40 sec sampling interval. This gave reasonably good results, standard deviations were 210 m and 224 mm/s (range only). Range rate was a better data type (74 m and 58 mm/s). Results with combined data gave 66 m and 52 mm/s.

Variable	Standard Deviation		
	Range	Range-Rate	Combined
x_1	.001 km	.003 km	.001 km
y_1	.008 km	.008 km	.008 km
z_1	.010 km	.010 km	.010 km
$\dot{x}_1$	.001 m/s	.001 m/s	.001 m/s
$\dot{y}_1$	.000 m/s	.000 m/s	.000 m/s
$\dot{z}_1$	.001 m/s	.001 m/s	.001 m/s
x_2	.003 km	.002 km	.002 km
y_2	.003 km	.002 km	.002 km
z_2	.002 km	.001 km	.001 km
$\dot{x}_2$	.002 m/s	.001 m/s	.001 m/s
$\dot{y}_2$	.002 m/s	.001 m/s	.001 m/s
$\dot{z}_2$	.003 m/s	.002 m/s	.002 m/s

Case 4: Standard Deviations - 10 m ATS A Priori

Table 11

Case 5: Several runs were made to explore the effect on GEOS recovery of larger ATS errors. These runs are 1 hour arcs and thus can be directly compared with Case 4, where results were:

	σ_x	σ_y	σ_z
range	165 m	210 m	24 m
r - r	9 m	74 m	15 m
comb	9 m	66 m	13 m

When σ_x was increased from 10 m to 1000 m, the results became:

r	172 m	218 m	24 m
r - r	9 m	207 m	41 m
comb	9 m	69 m	14 m

When σ_y was increased to 1000 m, the results were:

r	171 m	361 m	53 m
r - r	10 m	238 m	47 m
comb	90 m	158 m	31 m

When σ_z of ATS was increased from 10 m to 1000 m, the results were:

r	182 m	215 m	28 m
r - r	153 m	75 m	73 m
comb	27 m	75 m	23 m

Because of the complicated geometry it is difficult to explain the effects of the individual components.

When the relay apriori was increased from 10 m and 1 mm/sec to 100 m and 10 mm/sec at one time, the results were:

r	174 m	690 m	133 m
r - r	21 m	229 m	46 m
comb	20 m	227 m	45 m

It is clear that range rate is a better measurement type than range, particularly when the ATS errors are small. In this configuration it does not appear that one can say that range-rate is less sensitive to ATS errors than is the range data, (see Series I, Cases 6 and 7).

An Example of Equivalence

Lack of complete observability means that there is some combination of position and velocity components which cannot be determined from the data. This implies that the state vectors leading to a given measurement sequence are not unique. That is, the satellite state vectors can be perturbed and still generate the same measurement sequence.

To verify this property of unobservability, we took the orbits of ATS-6 and GEOS-C from May 2, 1975, 23 hr. 30 min. to May 2, 24 hr, 0 min. and used the idealized analysis program to develop a direction in 12-space which was unobservable over this half-hour arc. This direction is given by the following vectors:

$$\Delta\, pos_1 = [70239.03 \quad 38673.52 \quad 20260.21\text{m}]$$
$$\Delta\, vel_1 = [-2.912502 \quad 5.043442 \quad -.2959665\text{m/sec}]$$
$$\Delta\, pos_2 = [11233.49 \quad 6944.440 \quad 3138.174\text{m}]$$
$$\Delta\, vel_2 = [1.646808 \quad -2.278966 \quad 0]$$

When this increment of state was entered in the real-word simulation model (not the idealized model), changes in sensor readings occurred of about 0.2mm/sec in range rate and about 135m in range. These differences were constant over the arc. When this increment was increased by a factor of ten, the sensor discrepancies jumped to about 13mm/sec and 15000m, indicating that the changes are nonlinear effects.

Appendix A

Lemma: $(A'A)^{\dagger} = A^{\dagger}A'^{\dagger} = A^{\dagger}A^{\dagger\prime}$.

Proof: We show that it satisfies the four Penrose Axioms.

3) $(A'A)^{\dagger}A'A$ is symmetric

$$A^{\dagger}A'^{\dagger}A'A = A^{\dagger}(AA^{\dagger})'A = A^{\dagger}AA^{\dagger}A$$
$$= A^{\dagger}A$$

which is symmetric.

4) $A'A(A'A)^{\dagger}$ is symmetric. To show this, we recall that

$$B^{\dagger}BB' = B$$

and

$$B'^{\dagger} = B^{\dagger\prime} .$$

Then

$$A'AA^{\dagger}A'^{\dagger} = A'A'^{\dagger} = (A^{\dagger}A)'$$

which is symmetric.

1) $A'A(A'A)^{\dagger}A'A = A'A$
$= A^{\dagger}AA'A$ from 4) above
$= A'A$

2) $(A'A)^{\dagger}A'A(A'A)^{\dagger} = (A'A)^{\dagger}$
$= A^{\dagger}AA^{\dagger}A'^{\dagger}$ from 3) above
$= A^{\dagger}A'^{\dagger}$.

Appendix B

In this program, the primary method of calculating covariances, etc. is via the pseudo-inverse of the sensitivity matrix, rather than via the pseudo-inverse of the information matrix. Because this is not a typical procedure, we would like to outline the rationale for its use.

First, let us agree that in most instances, the technique is impractical since it requires the retention and processing of a matrix having dimensions of the number of measurements by the number of adjusted states. In addition, the treatment of a priori information is somewhat more complicated.

However the inversion process itself is numerically better conditioned. This fact can be illustrated in a number of ways.

First, consider a sensitivity matrix, S, which is N by n with N>>n. The information matrix, W = S'S, is n by n. It seems very reasonable that independence of n N-vectors will be easier to detect than independence of n n-vectors.

Second, note that for any symmetric matrix S, the eigenvalues of W = S'S are the squares of eigenvalues of S. While this does not hold for arbitrary square matrices, there is a tendency for the largest eigenvalue to more than square and the smallest to less than square, thus more than squaring the conditioning number (= max $|\frac{\lambda_i}{\lambda_j}|$).

Thirdly, some examples will illustrate the effect.

Example 1: Consider the nearly singular matrix

$$S = \begin{bmatrix} 1 & 1+\varepsilon \\ 1 & 1 \end{bmatrix} .$$

The eigenvalues are

$$\lambda_1 = 1 + \sqrt{1+\varepsilon} \approx 2$$

$$\lambda_2 = 1 - \sqrt{1+\varepsilon} \approx -\frac{\varepsilon}{2}$$

If gaussian elimination is used on this matrix then the second step finds the matrix

$$S_1 = \begin{bmatrix} 1 & 1+\varepsilon \\ 0 & -\varepsilon \end{bmatrix}$$

and the pivot element is $-\varepsilon$. The angle between the column vectors of this matrix is approximately

$$\alpha = \sin^{-1} \frac{\varepsilon}{\sqrt{4+4\varepsilon+2\varepsilon^2}}$$

(This criterion is of interest when using a Gram-Schmidt procedure for inversion, and is particularly attractive because it can be applied to nonsquare matrices.)

The matrix

$$W = S'S = \begin{bmatrix} 2 & 2+\varepsilon \\ 2+\varepsilon & 2+2\varepsilon+\varepsilon^2 \end{bmatrix}$$

has eigenvalues which are approximately given by

$$\mu_1 = 4 + 2\varepsilon + \varepsilon^2$$

$$\mu_2 = \varepsilon^2 .$$

If gaussian elimination is used on this matrix then the second step finds the matrix

$$W_1 = \begin{bmatrix} 2 & 2+\varepsilon \\ 0 & \frac{\varepsilon^2}{2} \end{bmatrix}$$

and the pivot element is $\frac{\varepsilon^2}{2}$.

This means that results which are obtained from single precision operations on S can be achieved using W only by forming W and operating on it in double precision.

The angle between the column vectors of W is approximately

$$\rho = \sin^{-1} \frac{\varepsilon^2}{8} ,$$

which leads to the same conclusions.

Example 2: Consider the 2Nx2 sensitivity matrix

$$S = \begin{bmatrix} 1 & 1+\varepsilon \\ 1 & 1-\varepsilon \\ & \equiv \\ 1 & 1+\varepsilon \\ 1 & 1-\varepsilon \end{bmatrix}$$

The angle between the column vectors is approximately

$$\alpha = \sin^{-1}\varepsilon \quad .$$

When the information matrix

$$W = S'S = \begin{bmatrix} 2N & 2N \\ 2N & 2N(1+\varepsilon^2) \end{bmatrix}$$

is formed, the angle between the vectors is essentially squared and the inversion difficulty is increased.